Size- and Strain-Dependent Electronic Structures in H-Passivated Si [112] Nanowires

ARTICLE *in* THE JOURNAL OF PHYSICAL CHEMISTRY C · SEPTEMBER 2008

Impact Factor: 4.77 · DOI: 10.1021/jp802591v

6 AUTHORS, INCLUDING:

Ning Lu
Chinese Academy of Agricultural Sciences
162 PUBLICATIONS **2,074** CITATIONS
SEE PROFILE

Jia-An Yan
Towson University
37 PUBLICATIONS **749** CITATIONS
SEE PROFILE

Size- and Strain-Dependent Electronic Structures in H-Passivated Si [112] Nanowires

Li Huang,*,†,‡ Ning Lu,†,§ Jia-An Yan,‡ M. Y. Chou,‡ Cai-Zhuang Wang,†,§ and Kai-Ming Ho†,§

U.S. Department of Energy, Ames Laboratory, Ames, Iowa 50011, School of Physics, Georgia Institute of Technology, Atlanta, Georgia 30332, and Department of Physics, Iowa State University, Ames, Iowa 50011

Received: March 25, 2008; Revised Manuscript Received: July 20, 2008

Using first-principles calculations within density functional theory, we have investigated the electronic properties of H-passivated Si nanowires (SiNWs) oriented along the 112 direction, with the atomic geometries retrieved via global search using genetic algorithm. We show that [112] SiNWs have an indirect band gap in the ultrathin diameter regime, whereas the energy difference between the direct and indirect fundamental band gaps progressively decreases as the wire size increases, indicating that larger [112] SiNWs could have a quasi-direct band gap. We further show that this quasi-direct gap feature can be enhanced when applying uniaxial compressive stress along the wire axis. Moreover, our calculated results also reveal that the electronic band structure is sensitive to the change of the aspect ratio of the cross sections.

Si nanowires (SiNWs) have attracted great attention as they could be one of the most promising building blocks for future nanoscale devices due to their compatibility with currently well developed Si-based technology. Recent experimental results have already demonstrated applications of SiNWs as electrical devices, including field-effect transistors,[1−3] p−n junctions,[4] and chemical and biological sensors.[5,6] This wide range of applications can be achieved because of their novel electronic and optical properties arising from the quantum confinement, which allows for modifications by precise control of the wire structures and stoichiometries during synthesis and manufacturing processes, for example, the thickness, crystal orientation, surface passivation, and doping.

A detailed understanding of the electronic properties of SiNWs and the various possible ways to modify it are of primary importance to the development of new applications. It could be extremely difficult to get this information from experiments. To our knowledge, so far only one experimental work has been reported on the study of the orientation and diameter dependence of the electronic band gap of SiNWs.[7] However, the interpretation of the experimental observations is still up for some debate and needs further verification from calculations. A number of computational studies have been devoted to address the structure−property relationship in hydrogenated SiNWs, mostly on [001], [110], and [111] oriented NWs,[8−12,14,13] whereas much less attention has been paid to [112] SiNWs,[15,16] although most of the experimental measurements of the electronic band gap are available for this growth orientation. Moreover, almost all previous studies just used heuristically proposed NW structures as a starting point.

Recently, we have employed a genetic algorithm (GA) approach[17] combined with density functional theory (DFT) calculations to determine the structures of ultrathin H-passivated SiNWs oriented along the [112] directions.[18,19] We found that the cross sections of the [112] SiNWs are perfectly rectangular bounded by monohydrated {110} and {111} facets with dihydride edges. The aspect ratio of the cross section of the magic wire geometries retrieved by the GA-DFT optimization procedure in the ultrathin diameter regime cannot be predicted by the thermodynamic considerations based on the Wulff construction.[20]

In this paper, we focus our investigation on the modification of electronic properties of H-passivated SiNWs oriented along the [112] direction. We study, using first-principles calculations, (1) how the electronic structures evolve as the number of atoms per unit length increases with diameters ranging from subnanometer to 3 nm, (2) the effects of the uniaxial strain along the wire axis on its band structure, and (3) how the electronic band structure responds to the change of the aspect ratio of the cross section of SiNWs.

Our calculations are carried out using the VASP code[21] based on DFT with ultrasoft pseudopotenitals[22] and plane-wave basis sets. The exchange-correlation functional is treated within the local density approximation (LDA). The energy cutoff for plane waves is set equal to 19 Ry. One primitive unit cell of the wire is used to create an effectively infinite wire by periodic repetition of this unit cell along the wire axis. More than 18 Å vacuum space is used in lateral directions to avoid any interactions between the image NWs in neighboring cells. Five Monkhorst−Pack[23] k points are used to sample the essentially one-dimension Brillouin zone along the wire axial direction. The atomic positions and lattice parameters along the wire axis are then fully optimized with no symmetry constraints until the forces on each atom become less than 0.01 eV/Å, and the total energy converged to the order of 10^{-4} eV per cell. Tests have been performed to make sure that all of the results are fully converged with respect to the energy cutoff, k-point sampling, and vacuum spacing.

As is well-known, the conventional DFT-LDA calculations suffer from the systematic underestimation of the band gap. In this work, the LDA gaps at the Γ point in two thinnest SiNWs are therefore rectified by using the many-body perturbation method based on the *GW* approximation,[24] which is highly computationally intensive, especially for larger diameter wires. The technical details of the *GW* calculations can be found in ref 14. The *GW* corrections increase the gap to the approximately correct value. Nevertheless, the general trend of the band gap variation as a function of the wire size and the energy dispersion

* To whom correspondence should be addressed.
† Ames Laboratory.
‡ Georgia Institute of Technology.
§ Iowa State University.

10.1021/jp802591v CCC: $40.75
Published on Web 09/13/2008

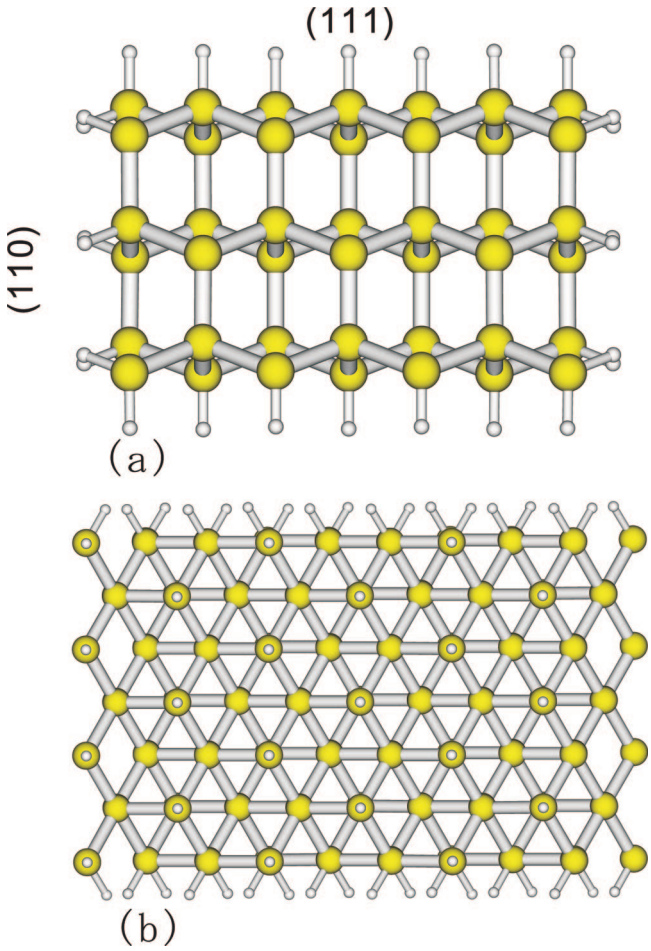

Figure 1. (a) Top view and (b) side view of the (7,3) SiNW, corresponding to $M = 7$ planes parallel to (110) and $N = 3$ complete (111) bilayers. Passivating hydrogen atoms are shown by small spheres.

TABLE 1: Diameter (d, in nm) and the Number of Si and H Atoms in the Unit Cell for the [112] SiNWs Obtained by a Global Genetic Search and Investigated in This Work

(M,N)	d	Si	H	(M,N)	d	Si	H
(4, 2)	0.85	16	16	(9, 4)	1.73	72	34
(5, 2)	0.95	20	18	(8, 5)	1.81	80	36
(6, 2)	1.03	24	20	(10,5)	2.02	100	40
(5, 3)	1.14	30	22	(11,5)	2.12	110	42
(7, 3)	1.34	42	26	(10,6)	2.21	120	44
(7, 4)	1.53	56	30	(12,7)	2.60	164	52
(8, 4)	1.63	64	32	(14,8)	2.98	224	60

close to the gap region are reliably reproduced by the DFT-LDA calculations.[25]

Following our previous work in ref 19, the geometry of [112] SiNWs are characterized by the number of (110) layers (M) and the number of complete (111) bilayers (N). Here we denote this as an (M,N) wire. Shown as an example in Figure 1 is the top and side views of the geometric structure of the (7,3) wire. In Table 1, we summarize the diameters and stoichiometries of the selected magic wires retrieved by the global genetic search. The diameter of each (M,N) wire is determined by $d = 2(A/\pi)^{1/2}$, where A is the area of the rectangular cross section of the H-passivated SiNWs. As can been seen in Table 1, the aspect ratio ($M \times d_{110}$:$N \times d_{111}$) of the cross-section of the magic wires does not vary monotonically in the ultrathin diameter regime, and is not given by the thermodynamic Wulff construction,[19] which predicts that the distance from the wire axis to any given

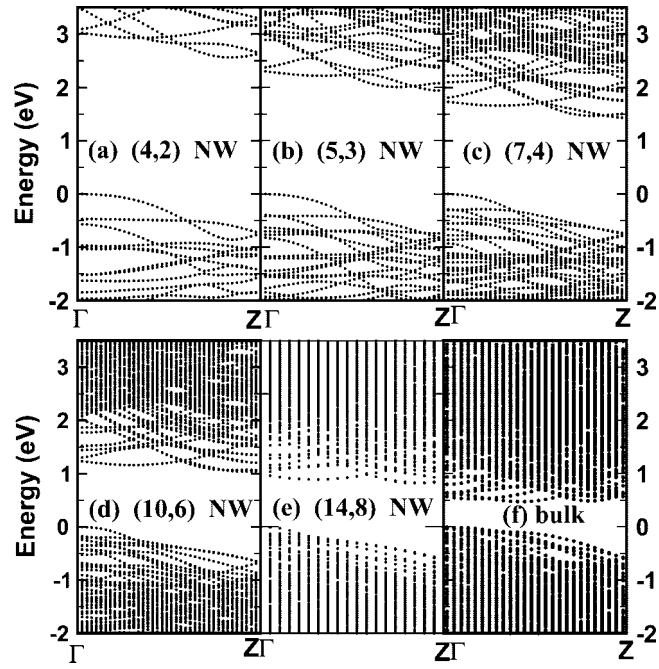

Figure 2. Energy band structures of selected [112] SiNWs: (a) (4,2) NW with $Si_{16}H_{16}$; (b) (5,3) NW with $Si_{30}H_{22}$; (c) (7,4) NW with $Si_{56}H_{30}$; (d) (10,6) NW with $Si_{120}H_{44}$; and (e) (14,8) NW with $Si_{224}H_{60}$. (f) The band structure of bulk Si projected in the [112] direction. The energy zero is set arbitrarily at the valence band maximum (VBM).

facet is strictly proportional to the surface energy of the facet orientation. Band structure calculations are then performed for these fully relaxed geometries.

Several typical band structures for the [112] SiNWs are shown in Figure 2. The overall features of the band structure for the other wires investigated are quite similar. The energy dispersion near the gap region of [112] SiNWs is characterized by the well-resolved valence band maximum (VBM) at the Γ point and the conduction band minimum (CBM) near the Z point (zone edge), leading to an indirect nature of the band gaps. This is in sharp contrast to the band gaps of [100], [110], and [111] SiNWs, all of which exhibit a transition to direct band gaps in the same diameter regime.[13,14,28] A projected band structure from the bulk is also shown for comparison. When the bulk bands are projected along the [112] direction, quite a few high-symmetry points are projected to the center of the one-dimensional Brillouin zone, including X, L, K, W, and U. Other L and X points are projected to the zone boundary Z. It turns out the six conduction band minima are projected to two different locations in the one-dimensional Billouin zone [see Figure 2f]. When the rectangular wires are formed, confinement effects are different for the two sides, raising one minimum more than the other, but the feature of an indirect band gap remains.

Figure 3 shows the size dependence of the direct and indirect band gaps, together with the GW -corrected direct band gaps for the (4,2) and (5,2) wire. As expected from the quantum confinement effect, the band gap generally decreases with increasing wire size. The GW corrections for the two thinnest [112] wires turn out to be 2.17 eV (= 5.16−2.99) and 2.14 eV (= 4.80−2.66), respectively. These are much larger than that found in the bulk, which is about 0.5 eV (= 1.08−0.58). This finding thus supports our previous observations in SiNWs grown in other orientations that the self-energy correction is strongly enhanced with decreasing wire size.[13,14]

Also shown in Figure 3 are the band gaps of [112] wires measured by tunneling spectroscopy.[7] For a better comparison

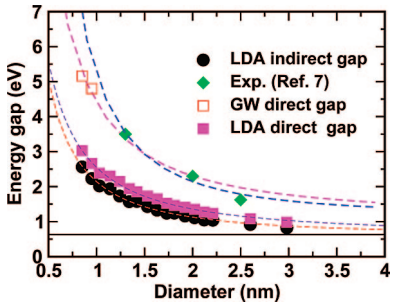

Figure 3. Calculated indirect (solid circles) and direct (solid squares) energy band gaps with LDA and direct band gaps with GW (empty squares) versus the diameter for [112] SiNWs. For comparison the measured band gaps of [112] wires by Ma et al.[7] (diamonds) are plotted. The solid horizontal line indicates the LDA gap of bulk Si. The dashed lines is fitted to the data points (see text). The fitting results are listed in Table 2.

TABLE 2: Fitting Parameters for Theoretical and Experimental Band Gaps As a Function of Diameter[a]

parameter	LDA (indirect)	LDA (direct)	GW	exp.[7]
C	1.56	1.97	3.32	4.04
α	1.51	1.35	1.44	2.06

[a] The fitting has included the corresponding bulk value as the limit.

between the experimental and calculated band gaps, we fit the calculated (measured) data points with an approximate function of $E_{g,bulk} + C(1/d)^{\alpha}$,[26] where $E_{g,bulk}$ is the corresponding bulk gap value and C and α are fitting parameters. The diameter exponent $\alpha \simeq 2$ for the experimental values is in accordance with the prediction by using an effective-mass particle-in-a-box model with an infinite barrier height. The α value is smaller for the calculated data (see fits in Figure 3 and Table 2). It is apparent that the dependence of the *GW* gaps on the wire size is somewhat different as compared with the experimental results. Nevertheless, it is important to note that the LDA gaps follow closely their *GW* counterparts. In addition, the quantitative difference here might also be attributed in part to the facts that the fitting procedures are based on only a few data points and that the definition of the wire diameters is somehow arbitrary. It is also noted that the diameter quoted in ref 7 is likely to be the width of the (111) facet, instead of the "effective diameter" defined by the cross-sectional area used in Figure 3. Therefore, the experimental points may not be plotted correctly according to the definition of diameter used in this paper.

Besides the indirect band gap, we also analyze the direct gap at Γ point, which is more relevant to the optoelectronic applications for SiNWs. For comparison purposes, the direct fundamental band gap is also included in Figure 3. It is interesting to observe that the energy difference between the direct and indirect fundamental gaps progressively decreases as the wire size increases. This feature can be traced back to the band structure of bulk Si projected in the [112] direction since the band gap and band edge states of a large SiNW with a small surface−volume ratio involved should develop toward its asymptotic bulk value. As shown in Figure 2f, the energy difference of the direct and indirect band gaps is only 0.1 eV in the projected band structure. This trend suggests that the larger [112] SiNWs could have a quasidirect band gap. We note that this feature has also been found in other two studies very recently.[15,16]

We now proceed to show that uniaxial stress may have an effect on the relative size of the direct and indirect band gaps.

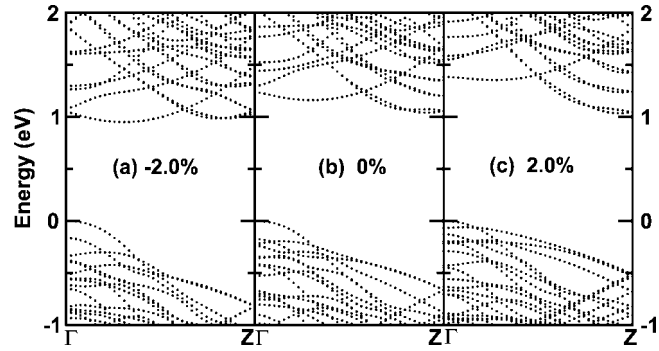

Figure 4. Energy band structures of the (10,6) SiNW with a diameter of 2.21 nm: (a) with 2% compressive strain along the wire axis; (b) free of axial strain; and (c) with 2% tensile strain along the wire axis. The strain is defined as the ratio of the lattice constant of a strained SiNW to that of a strain-free SiNW. The VBM has been shifted to zero.

Presented as an illustrative example in panels a−c in Figure 4 are the band structures of the (10,6) wire under compressive, zero, and tensile uniaxial stress, respectively. It is evident that the energy difference between the indirect fundamental band gap and the direct one reduces with the increase of the compressive strain. This observation is also valid for other [112] SiNWs with different diameters. Starting from the projected band structure from the bulk, where the direct and indirect band gaps differ by only 0.1 eV, the rectangular confinement breaks the local cubic symmetry, and, in most cases we studied, raises the direct band gap more than the indirect one. The axial strain in turn adds another variational degree of freedom in changing the relative magnitude of these gaps. Similarly, varying the aspect ratio may accomplish the same effect.

As we have mentioned earlier, the aspect ratio of the rectangular cross section is not solely dictated by the ratio of surface energies as would be expected from the Wulff construction in the thin NWs where most of the atoms are at the surface. It is thus interesting to explore how the interplay between the relative number of atoms on the [111] and [100] surfaces modifies, if possible, the electronic properties of the nanowires. To evaluate the effects of different aspect ratios of the cross section of SiNWs on its band structure and band gaps, we have performed calculations on the (4,8) and (16,2) wires, which are not energetically favorable wire geometries as compared to the (8,4) wire (the magic wire of the same 64 Si atoms per unit length). The resulting electronic structures are shown in Figure 5. It can be seen that the three [112] SiNWs with quite different aspect ratios do show noticeable differences in their band structures, as far as both band gap energy and dispersions of valence and conduction band are concerned. The (4,8) SiNW even shows a clear direct band gap, essentially different from the indirect band gap feature of the (8,4) and (16,2) SiNWs. It is noted that this observation for the [112] wire here is in good agreement with the finding by Migas in ref 27, where the [100] SiNWs with similar diameters but different cross sections were found to have distinctly different band gap size. However, we also note that this is not the case for the [110] wire according to the calculations by Ng et al. in ref 28, where they found that the different patterns of the cross section did not cause significant band gap changes for those [110] SiNWs with the same cross-sectional area.

In summary, the electronic properties of H-passivated [112] SiNWs with the atomic geometries retrieved via the global

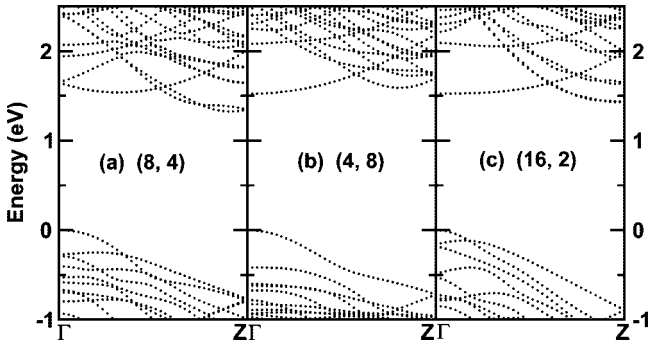

Figure 5. Representative energy band structures of SiNWs with the same number of Si atoms ($2MN = 64$) but different aspect ratios ($M \times d_{110}$:$N \times d_{111}$) of (a) 1.21, (b) 0.37, and (c) 4.60, respectively. The diameters are about 1.6 nm. The VBM has been shifted to zero.

search using genetic algorithm are investigated from first-principles calculations. We show that [112] SiNWs have an indirect band gap in the ultrathin diameter regime, whereas the energy difference between the indirect fundamental band gap and the direct one progressively decreases as the wire size increases, indicating that relatively thick [112] SiNWs could have a quasi-direct band gap. We further show that this quasidirect gap feature can be enhanced when applying uniaxial compressive stress along the wire axis. Moreover, our calculated results also reveal that the electronic band structure of SiNWs is sensitive to the change of the aspect ratio of the cross sections. These findings could have important implications for the use of SiNWs in nanoscale devices as experimentally [112] nanowires have been found to grow abundantly with application-relevant thicknesses.

Acknowledgment. Ames Laboratory is operated for the U.S. Department of Energy by Iowa State University under Contract No. DE-AC02−07CH11358. This work was also supported by the National Science Foundation (Grant No. DMR-02−05328) and the Department of Energy (Grant No. DE-FG02−97ER45632 and Computational Materials Science Network). The computation used resources of the National Energy Research Supercomputing Center (NERSC), which is supported by the Department of Energy (Grant No. DE-AC03−76SF00098), and the San Diego Supercomputer Center (SDSC).

References and Notes

(1) Cui, Y.; Zhong, Z.; Wang, D.; Wang, W. U.; Lieber, C. M. *Nano Lett.* **2003**, *3*, 149.
(2) Koo, S. M.; Li, Q. L.; Edelstein, M. D.; Richter, C. A.; Vogel, E. M. *Nano Lett.* **2005**, *5*, 2519.
(3) Goldberger, J.; Hochbaum, A. I.; Fan, R.; Yang, P. D. *Nano Lett.* **2006**, *6*, 973.
(4) Cui, Y.; Lieber, C. M. *Science* **2001**, *291*, 851.
(5) Cui, Y.; Wei, Q. Q.; Park, H. K.; Lieber, C. M. *Science* **2001**, *293*, 1289.
(6) Hahm, J.; Lieber, C. M. *Nano Lett.* **2003**, *4*, 51.
(7) Ma, D. D. D.; Lee, C. S.; Au, C. K.; Tong, S. Y.; Lee, S. T. *Science* **2003**, *299*, 1874.
(8) Vo, T.; Williamson, A. J.; Galli, G. *Phys. Rev. B* **2006**, *74*, 45116.
(9) Ponomareva, I.; Menon, M.; Richter, E; Andriotis, A. N. *Phys. Rev. B* **2006**, *74*, 125311.
(10) Niquet, Y. M.; et al. *Phys. Rev. B* **2006**, *73*, 165319.
(11) Li, J.; Freeman, A. J. *Phys. Rev. B* **2006**, *74*, 75333.
(12) Rurali, R.; Lorente, N. *Phys. Rev. Lett.* **2005**, *94*, 26805.
(13) Zhao, X.; Wei, C. M.; Yang, L.; Chou, M. Y. *Phys. Rev. Lett.* **2004**, *92*, 236805.
(14) Yan, J. A.; Yang, L.; Chou, M. Y. *Phys. Rev. B* **2007**, *76*, 115319.
(15) Lu, A. J.; Zhang, R. Q.; and Lee, S. T. *Nanotechnology* **2008**, *19*, 35708.
(16) Rurali, R.; Aradi, B.; Frauenheim, T.; Gali, A. *Phys. Rev. B* **2007**, *76*, 113303.
(17) Ho, K. M.; Shvartsburg, A. A.; Pan, B. C.; Lu, Z. Y.; Wang, C. Z.; Wacker, J.; Fye, J. L.; Jarrold, M. F. *Nature* **1998**, *392*, 582.
(18) Chan, T. L.; Ciobanu, C. V.; Chuang, F. C.; Lu, N.; Wang, C. Z.; Ho, K. M. *Nano Lett.* **2006**, *6*, 277.
(19) Lu, N.; Ciobanu, C. V.; Chan, T. L.; Chuang, F. C.; Wang, C. Z.; Ho, K. M. *J. Phys. Chem. C* **2007**, *111*, 7933.
(20) Pimpinelli, A.; Villain, J. *Physics of Crystal Growth*; Cambridge University Press: New York, 1998; Chapter 3.
(21) Kresse, G.; Hafner, J. *Phys. Rev. B* **1994**, *49*, 14251. Kresse, G.; Furthmüller, J. *Comput. Mater. Sci.* **1994**, *6*, 15.
(22) Vanderbilt, D. *Phys. Rev. B* **1990**, *41*, 7892. Kresse, G.; Hafner, J. *J. Phys.: Condens. Matter* **1994**, *6*, 8245.
(23) Monkhorst, H. J.; Pack, J. D. *Phys. Rev. B* **1976**, *13*, 5188.
(24) Hybertsen, M. S.; Louine, S. G. *Phys. Rev. B* **1986**, *34*, 5390, and references therein.
(25) Williamson, A. J.; Grossman, J. C.; Hood, R. Q.; Puzder, A.; Galli, G. *Phys. Rev. Lett.* **2002**, *89*, 196803.
(26) Delerue, C.; Allan, G.; Lannoo, M. *Phys. Rev. B* **1993**, *48*, 11024.
(27) Migas, D. B. *J. Appl. Phys.* **2005**, *98*, 54310.
(28) Ng, M. F.; Zhang, L.; Yang, S. W.; Sim, L. Y.; Tan, V. B. C.; Wu, P. *Phys. Rev. B* **2007**, *76*, 155435.

JP802591V